

Simulating Magnets with One-Dimensional Ising Models

Alice Heiman
`alice.l.heiman@gmail.com`

under the direction of
Andrea Ludovico Benfenati
Department of Condensed Matter Physics
KTH Royal Institute of Technology

Research Academy for Young Scientists
July 14, 2021

Abstract

This report implements and investigates the behavior of the one-dimensional Ising model with Monte Carlo simulations and analytical methods. The Ising model provides a way to capture and study core magnetic properties without performing time-consuming and expensive experiments in labs. Using the Metropolis-Hastings algorithm, a system of spins was subjected to different temperatures under the influence of various external magnetic fields. With each iteration, the spins were flipped. Depending on the change in energy resulting from every flip, they were then either rejected or accepted for the next iteration. The magnetization and energy density could then be computed and compared with other systems of different sizes. The results indicate that large one-dimensional systems do not have spontaneous magnetization. However, small system sizes show signs of magnetization at low temperatures. One-dimensional Ising models display many important magnetic properties and provide a basis on which more complex models can be built. Further developments include expanding the range of interactions between neighboring spins, investigating how multiple systems interact, and exploring possible parallels with group sociology.

Acknowledgements

I want to express my gratitude to my mentor Andrea Ludovico Benfenati for his guidance, insights, and patience. It is truly incredible how much ground can be covered in solely two weeks. Special thanks to all organizers of Rays for their endless energy, support, and capability of handling even the strangest situations. To all previous Rays students, I cannot thank you enough for taking the time to give such detailed feedback. Finally, thank you Kjell & Märta Beijers Stiftelse, Kungl. Patriotiska Sällskapet, and Rays – For Excellence, for making this adventure possible.

Contents

1	Introduction	1
1.1	The 1D-Ising Model	1
1.1.1	System Energy	2
1.1.2	The Boltzmann Distribution and Free Energy	4
1.2	Specific Heat and Magnetic Susceptibility	6
1.3	Mean-Field Approximation	6
1.4	Exact Solution	8
1.5	Monte Carlo, Metropolis-Hasting, and Markov Chains	9
1.6	Literary Review	9
2	Method	10
2.1	Monte Carlo Simulations	10
2.2	Analytical Methods	13
3	Results	14
3.1	A Note on Units	14
3.2	Varying Temperatures without External Magnetic Fields	14
3.3	Varying Temperatures with External Magnetic Fields	16
3.4	Varying External Magnetic Field	17
3.5	Small Systems of Size $N < 100$	18
4	Discussion	22
4.1	Small Systems of Size $N < 1000$	23
4.2	Limitations	24
4.3	Applications and Further Development	24
	References	25
A	Appendix	26

1 Introduction

Reality often proves too complex to model with practicable computing power. The sheer scale of the universe quickly extinguishes the aspiration of deterministically simulating, for example, all particle interactions. Instead, simpler models can be used to emulate the main characteristics of their physical counterparts. They also provide full control of parameters, making it possible to experiment even beyond known physical limits and discover where current intuitions or models break down. These insights could indicate promising future research areas and shed light on where the understanding of today falters. Together with statistical methods, these techniques have become important in the field of theoretical and statistical physics. One such example is the simulation of magnetism, where computer models can give insights into real-world underlying mechanisms. [1]

1.1 The 1D-Ising Model

The Ising model is one of the simplest models used to study magnetic materials. It consists of a lattice of spins that can solely point up or down and interact with their immediate neighbors, as shown in Figure 1 [2]. A specific configuration of a system is defined as $\Omega_i = \{\sigma_1, \sigma_2, \sigma_3, \dots, \sigma_N\}$, where every configuration is a particular composition of upward and downward spins.

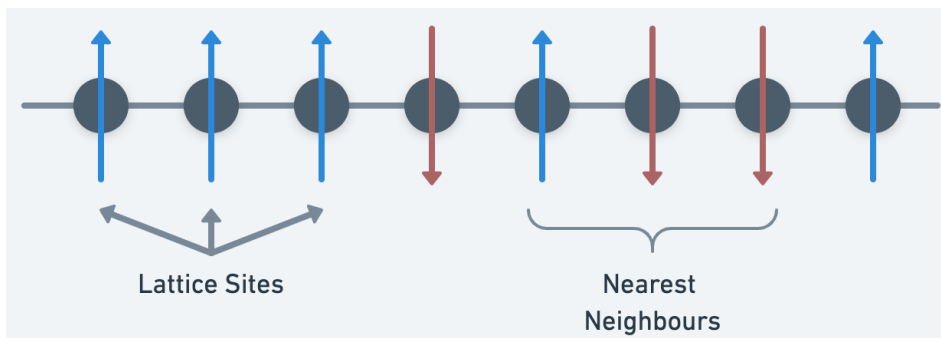


Figure 1: The Ising model is composed of N lattice sites with bidirectional spins. In one dimension, every spin, except those at the free ends, has two neighbors. Blue arrows indicate upward spins, and red arrows represent downward spins.

Every spin act as a miniature magnet and possesses a *magnetic moment* whose orientation either contributes to or counteracts the total magnetic field. The combined strength of the spontaneous magnetic field is called *magnetization*, denoted m . The magnetization of a specific system is written $m(\Omega_i)$. In *ferromagnets*, the magnetic moments tend to align naturally, which increases the magnetization of the system. Other materials, called *paramagnets* and *diamagnets*, have magnetic moments that only align in response to external magnetic fields. Systems having zero magnetization, due to spins aligning in an orientation opposite that of their neighbors, are said to be *antiferromagnetic*, see Figure 2. [3]

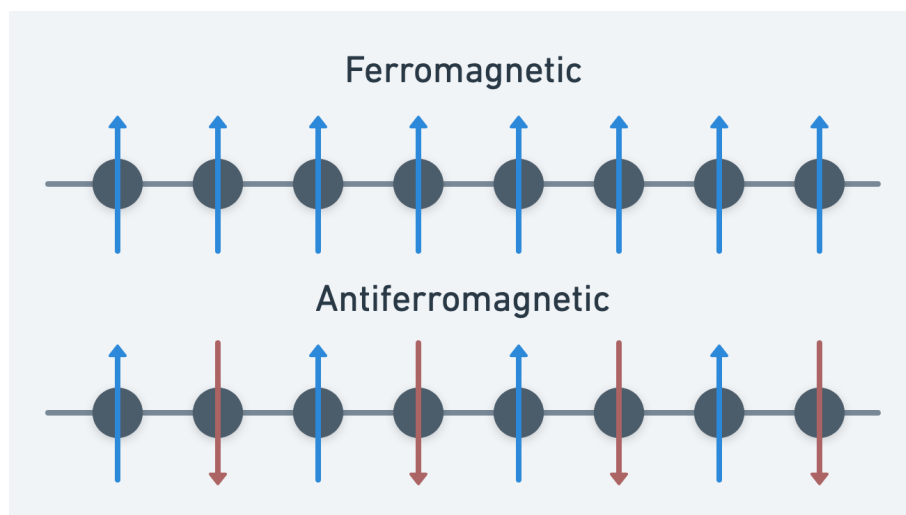


Figure 2: In ferromagnetic materials, all spins point in the same direction, amplifying the total magnetic field. In antiferromagnetic materials, all spins instead point in opposite directions, canceling out the overall magnetic field.

1.1.1 System Energy

Each spin is only affected by its nearest neighbors, where the *interspin exchange constant* J , determines the strength of the interactions. Every system tends towards a ground state, where the total energy is the lowest. The product of two magnetic moments and $-J$, gives the contribution of the two magnetic moments to the magnetization of the system, as in Equation (1):

$$\mathcal{H}(\sigma_i\sigma_{i+1}) = -J\sigma_i\sigma_{i+1}. \quad (1)$$

Spins in the same direction are favorable and contribute negative energy to the system, while spins in opposite directions instead contribute positive energy, as seen in Figure 3.



Figure 3: An upward spin has the value 1, while a downward spin has the value -1. The product of two spins in the same direction multiplied by a negative constant will always yield a negative energy contribution. The product of two opposite spins multiplied by a negative constant will instead yield a positive energy contribution.

A *bounded system* is a lattice with free ends, while an *unbounded system* is one of infinite size that can be simulated using the *periodic boundary condition*, denoted λ [1]. If $\lambda = 0$, the system is bounded and is said to have an *open boundary condition*, and a system is unbounded if $\lambda = 1$. Accounting for external magnetic fields, which is the sum of the spins multiplied by the field strength h , the system energy is described by Hamiltonian \mathcal{H} given by

$$\mathcal{H} = -J \sum_{i=1}^{N-1} \sigma_i \sigma_{i+1} + \lambda(-J\sigma_N\sigma_1) - h \sum_{i=1}^N \sigma_i, \quad (2)$$

where J is the interspin exchange constant, σ_i the value of the spin at lattice site i , λ the periodic boundary condition, and h the strength of an external magnetic field [1]. The first term of the right-hand side of the equation describes the energy between spins in a bounded system. The second part is the extra energy contribution from multiplying the last spin with the first, which is relevant in unbounded systems. A λ set to zero will ignore this part of the equation. The last term in (2) represents the energy contributed from an external magnetic field.

1.1.2 The Boltzmann Distribution and Free Energy

In reality, however, a system cannot reach its ground state. The outside temperature constantly provides energy that causes spins to flip. How many magnetic moments that flip is dependent on the temperature and through the *Boltzmann distribution*

$$p(E_{\Omega_i}) \propto e^{\frac{-E_{\Omega_i}}{k_B T}}, \quad (3)$$

where $p(E_{\Omega_i})$ is the probability of having a specific system, Ω_i , with energy E_{Ω_i} at temperature T [4]. The Boltzmann constant denoted k_B , which in this report is equal to one. The distribution is given up to proportionality and must be normalized for all probabilities to sum to one. Using C as a normalization constant equal to $\frac{1}{\sum_a e^{-E_a/k_B T}}$, where a is all possible system energies, the probability can be expressed as

$$p(E_{\Omega_i}) = C e^{\frac{-E_{\Omega_i}}{k_B T}}. \quad (4)$$

Interestingly enough, systems with different magnetizations can have the same probability, as they are only dependent on the temperature and system energy. A summary and examples of the terms magnetization, energy, and Boltzmann distribution probability are shown in Figure 4.

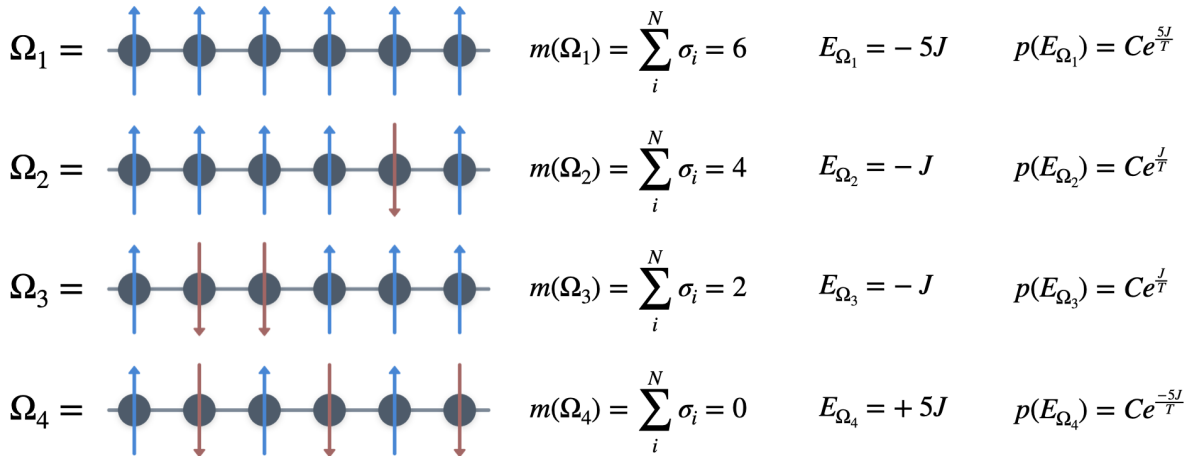


Figure 4: Examples of different system configurations and their magnetization, energy, and probability.

To account for system energies at temperatures above zero Kelvin, the change in *free energy* can be used as an extension of \mathcal{H} . It estimates when a system is prone to flip spins, eventually leading to an antiferromagnetic state, or when the system rather stays fixed in a ferromagnetic state. Helmholtz free energy, F , determined by

$$F = E - TS, \quad (5)$$

describes the free energy in the absence of an external magnetic field. Here, E is the internal energy, as determined by the Hamiltonian in Equation (2), T the temperature, and S the entropy of the system [2]. Entropy can be defined as the number of possible configurations of a system, denoted Ω_{conf} , as defined by (6) [2]:

$$S = k_B \log(\Omega_{\text{conf}}). \quad (6)$$

It is possible to examine the flip of the lowest energy cost to estimate the change in free energy. In a system with all spins aligned in the same direction, a lattice site can be selected from where all subsequent spins are flipped. This is called a *domain wall*, see Figure 5, and the energy change of this particular flip is $+2J$.

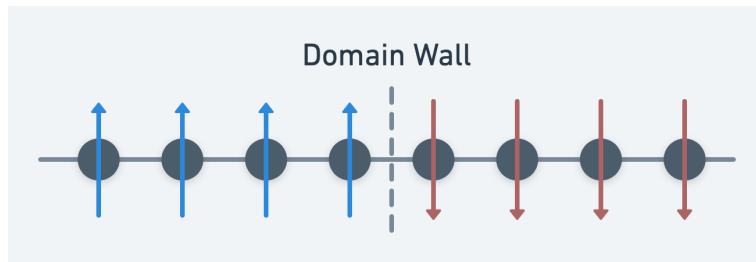


Figure 5: A domain wall separates two regions of unidirectional magnetic moments.

As the domain wall cannot be placed after the last spin in a bounded system, the number of domain wall configurations is $N - 1$. It is possible to describe the change in free energy with these values by:

$$\Delta F = \Delta E - TS = +2J - k_B T \log(N - 1). \quad (7)$$

According to the second law of thermodynamics, a system constantly tends to minimize its energy and maximize its entropy. Therefore, a negative change in free energy will always be favorable, causing the system to flip spins. On the other hand, a positive free energy change is less desirable, implying a lower probability for the system to flip.

1.2 Specific Heat and Magnetic Susceptibility

The *critical temperature* T_c is the temperature at which the system goes from being magnetized to being antiferromagnetic [2]. Specific heat and magnetic susceptibility can be used to find the critical temperature as these parameters often achieve their maxima at T_c . Heat capacity, C_v , is computed from the variance of the energy, denoted $\langle E^2 \rangle - \langle E \rangle^2$, as seen in Equation (8). However, heat capacity is an extensive quantity that will grow in response to the system size. Therefore, the heat capacity can be divided by the system size N to produce an intensive quantity. Dividing C_v by N gives the specific heat, seen in Equation 9. Magnetic susceptibility, χ , is computed with the variance in magnetization, denoted $\langle M^2 \rangle - \langle M \rangle^2$, which is shown in Equation (10). Here, $\beta = \frac{1}{k_B T}$, and the variances represent the standard deviations for the energy and magnetization, respectively. [1]

$$C_v = \frac{\beta}{T} (\langle E^2 \rangle - \langle E \rangle^2) \quad (8)$$

$$c_v = \frac{C_v}{N} \quad (9)$$

$$\chi = \beta (\langle M^2 \rangle - \langle M \rangle^2) \quad (10)$$

1.3 Mean-Field Approximation

There are multiple analytical approximations to the 1D-Ising model. The one covered in this report is the *mean-field approximation*. The mean-field approximation is based on two assumptions: (1) that the average magnetization of any one spin, denoted $\langle \sigma_1 \rangle$, is

equal to the total magnetization average, denoted $\langle m \rangle$, and (2) that fluctuations around the average can be ignored [1]. Starting with Equation (2), the energy of the spin at lattice site 1 is given by:

$$\mathcal{H}(\sigma_1) = -\sigma_1 \left(J \sum_{j=1}^q \sigma_j + h \right),$$

where q stands for the number of nearest neighbors to the spin σ_1 . Adding and subtracting the expression qJm does not alter the value of the above expression but includes the number of neighbors, q , the spin interaction, J , and the magnetization, m . Performing this arithmetic trick gives:

$$\begin{aligned} \mathcal{H}(\sigma_1) &= -\sigma_1 \left(J \sum_{j=1}^q \sigma_j + h + qJm - qJm \right) \\ &= -\sigma_1(qJm + h) - \sigma_1 J \sum_{j=1}^q (-qJm) \\ &= -\sigma_1(qJm + h) - J\sigma_1 \sum_{=1j}^q (\sigma_j - m). \end{aligned}$$

Using the no-fluctuation assumption, the second part of the expression can be discarded, which simplifies the expression to

$$\mathcal{H}(\sigma_1) = -\sigma_1(qJm + h).$$

Then a weighted average for the energy of spin σ_1 is computed. A weighted arithmetic mean is calculated by summing all values in the vector x_i multiplied by their weights in the weight vector, w_i , and then dividing by the sum of the weights [5].

$$\langle x_w \rangle = \frac{\sum_{i=1}^n w_i x_i}{\sum_{i=1}^n w_i} \quad (11)$$

The spins follow a Boltzmann distribution that is proportional to $e^{\frac{-E}{k_B T}}$. Using the Hamiltonian from Equation (2) for σ_1 , the expression simplifies to $e^{\beta H(\sigma_1)}$. In this case, the previously mentioned term determines the weight for the different states of σ_1 . As σ_1 takes on the values 1 and -1 , representing an upward and downward spin, the weighted average is the following:

$$\langle \sigma_1 \rangle = \frac{1 \cdot e^{\beta H(\sigma_1)} + (-1) \cdot e^{-\beta H(\sigma_1)}}{e^{\beta H(\sigma_1)} + e^{-\beta H(\sigma_1)}} = \frac{e^{\beta H(\sigma_1)} - e^{-\beta H(\sigma_1)}}{e^{\beta H(\sigma_1)} + e^{-\beta H(\sigma_1)}}.$$

The last expression follows the pattern for a hyperbolic tangent,

$$\tanh(x) = \frac{e^x - e^{-x}}{e^x + e^{-x}} \quad (12)$$

Therefore, it is possible to simplify the expression for the weighted average of the energy to:

$$\langle \sigma_1 \rangle = \tanh(\beta H(\sigma_1)).$$

Using $q = 2$, the expression for $H(\sigma_1)$, and the first assumption that $\langle \sigma_1 \rangle = \langle \sigma_i \rangle = \langle m \rangle$, a complete equation for the average magnetization is:

$$m = \tanh\left(\frac{2Jm + h}{T}\right). \quad (13)$$

1.4 Exact Solution

The 1D-Ising model also has an exact analytical solution given by

$$m = \frac{\sinh(\beta h)}{\sqrt{\sinh^2 \beta h + e^{-\beta J}}}, \quad (14)$$

where m is the magnetization, $\beta = \frac{1}{k_B T}$, h the strength of an external magnetic field, and J the interspin exchange constant [1].

1.5 Monte Carlo, Metropolis-Hasting, and Markov Chains

It is cumbersome to compute the effects of every individual particle in large systems. *Monte Carlo simulations* takes many random samples from the total and determines their average [2]. More iterations should, therefore, give a more representative approximation of reality. The simulations make it possible to attain very accurate approximations, although it was not possible to compute every single event.

The Metropolis-Hastings algorithm takes samples directly from a probability distribution when the normalizing constant is unknown. This way, it is unnecessary to take a weighted average, as in standard Monte Carlo methods. The one-dimensional Ising model follows the Boltzmann distribution proportional to $e^{-dE/T}$. In Metropolis-Hastings, candidates are repeatedly drawn from the distribution and then either rejected or accepted for the next round. Every iteration grows a series of states in which every state is only dependent on the previous, which is called a Markov Chain. A candidate is always accepted if the result of evaluating it with the distribution, α , is greater than one. However, if $0 < \alpha < 1$, the candidate is accepted with probability α and rejected with probability $1 - \alpha$. [6]

1.6 Literary Review

Ernst Ising created the Ising model in 1922, and it has since been studied and applied extensively [7]. In condensed matter physics, it allows scientists to study the properties of magnetic materials, lattice gases, and superconductors [7, 8]. Moreover, some use it as a simple socio-economic model to track, for example, segregation and language development [9]. The one-dimensional Ising model has also been implemented with quantum computers and solved exactly [10].

This study aims to use the one-dimensional Ising model to investigate the properties of magnets. Ernst Ising's exact solution states that no magnetization can occur without external magnetic fields. Nonetheless, this report will focus on minuscule temperatures

in the $0 < T < 16$ range and examine if spontaneous magnetization can arise in different-sized systems. Moreover, a great weight is placed on the implementation and efficiency of the algorithm to facilitate future research in multiple dimensions.

2 Method

All the code and graphs used for this paper can be found on GitHub with the following link: <https://github.com/aliceheiman/1d-ising-model>.

2.1 Monte Carlo Simulations

A system of N spins was initialized with all spins in random directions. Then a spin was flipped, and the resulting change in energy, dE , from the flip was computed. A random number, r , was then drawn with a value ranging from $0 < r < 1$. It was compared to the lowest value between one and $e^{-dE/T}$. If $r < \min(1, e^{-dE/T})$, the flip was accepted. Otherwise, it was rejected, and no change to the system was made for that iteration, see Figure 6. For example, if dE would be positive, the term $e^{-dE/T}$ would become very small. Therefore, r would be compared to this tiny number, resulting in a low probability for the flip to be accepted. On the other hand, a negative dE would give a large $e^{-dE/T}$. The minimum between one and $e^{-dE/T}$ would then be one. As r is always *less than* one, flips yielding a negative energy change would always get accepted.

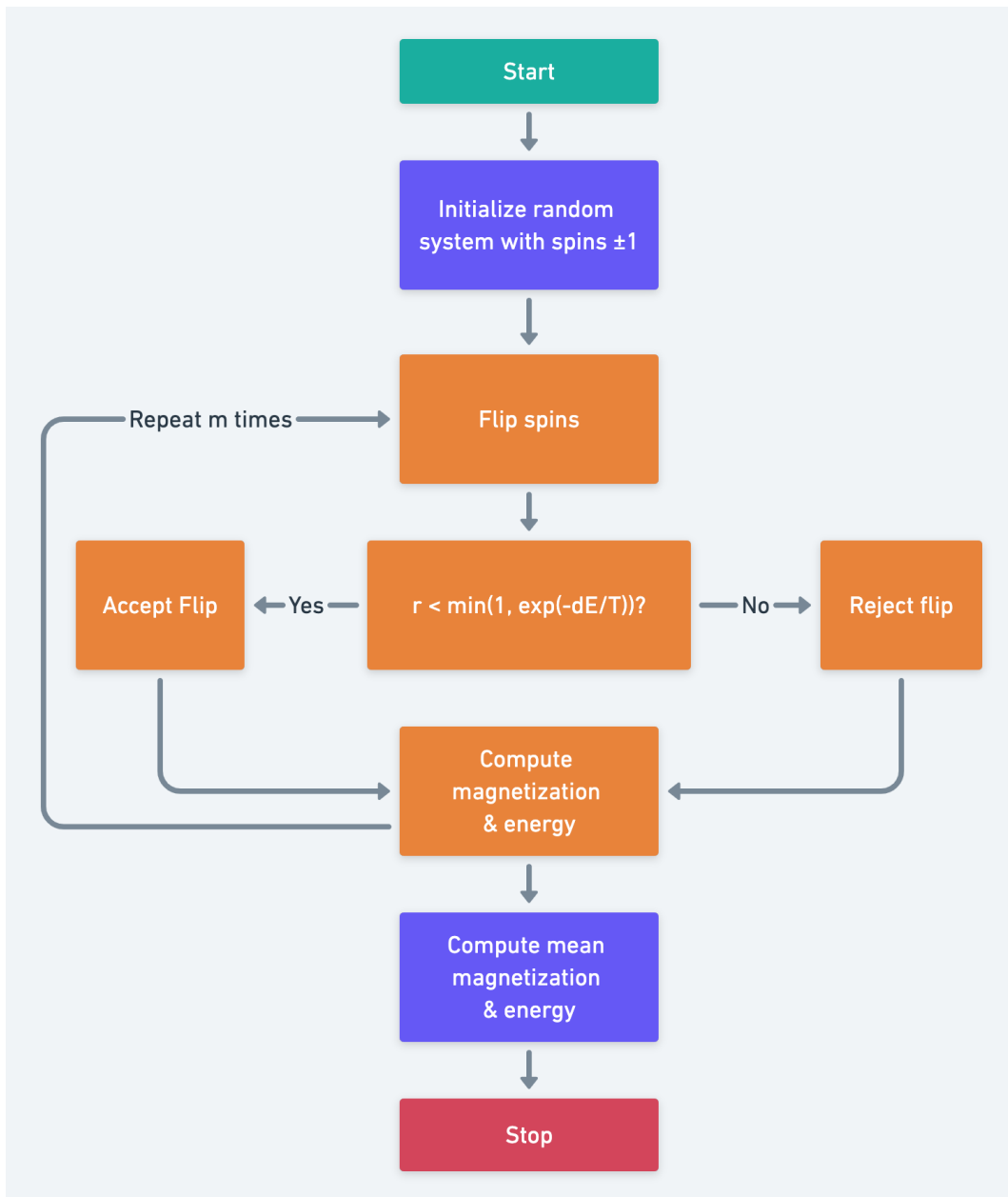


Figure 6: A schematic of the Metropolis-Hastings algorithm.

A great weight was placed on the implementation and efficiency of the algorithm. Instead of flipping only one magnetic moment with each iteration, the system was split into its even and odd spins, shown in Figure 7. As every spin is only affected by its two intermediate neighbors, it was possible to flip and examine the energy change of every other spin without disorienting the whole system.

$$\begin{array}{cccccc}
\textit{odd} & \textit{even} & \textit{odd} & \textit{even} & \textit{odd} & \textit{even} \\
\boxed{\sigma_1} & \boxed{\sigma_2} & \boxed{\sigma_3} & \boxed{\sigma_4} & \boxed{\sigma_5} & \boxed{\sigma_6} \\
\vec{\Omega}_E = \{\sigma_2, \sigma_4, \sigma_6\} & \vec{\Omega}_O = \{\sigma_1, \sigma_3, \sigma_5\}
\end{array}$$

Figure 7: The total system can be divided into two vectors, one containing all even lattice sites and the other all odd lattice sites.

To compute the change in energy of flipping all even spins in the system shown in Figure 7, it is possible to first consider the energy change of inverting the direction of σ_2 .

$$E_{old} = \mathcal{H}(\sigma_2) = -J(\sigma_2(\sigma_1 + \sigma_3)) - h\sigma_2$$

$$E_{new} = \mathcal{H}(-\sigma_2) = -J(-\sigma_2(\sigma_1 + \sigma_3)) + h\sigma_2$$

$$\begin{aligned}
dE &= E_{new} - E_{old} \\
&= -J(-2\sigma_2(\sigma_1 + \sigma_3)) + 2h\sigma_2 \\
&= 2J\sigma_2(\sigma_1 + \sigma_3) + 2h\sigma_2
\end{aligned}$$

Using the same expression for all even flips gives the following:

$$d\vec{E}_{\Omega_E} = \begin{bmatrix} 2J\sigma_2(\sigma_1 + \sigma_3) + 2h\sigma_2 \\ 2J\sigma_4(\sigma_3 + \sigma_5) + 2h\sigma_4 \\ 2J\sigma_6(\sigma_5 + \lambda\sigma_1) + 2h\sigma_6 \end{bmatrix}$$

where λ is the periodic boundary condition allowing a looping system. Notice how the first and last terms together in each expression constructs the even vector. The first terms within the parenthesis compose the odd vector, and the second terms constitute the odd vector shifted to the right by one. Applying this insight simplifies the expression to

$$d\vec{E}_{\Omega_E} = 2J\vec{\Omega}_E(\vec{\Omega}_O + \vec{\Omega}_{O\text{-shifted}}) + 2h\vec{\Omega}_E, \quad (15)$$

where the operations are an element-wise product and sum of vectors. Using the same logic, an expression for the change in energy of all odd spins is as follows:

$$d\vec{E}_{\Omega_O} = 2J\vec{\Omega}_O(\vec{\Omega}_{E\text{-shifted}} + \vec{\Omega}_E) + 2h\vec{\Omega}_O \quad (16)$$

With Equations (15) and (16), every iteration consisted of flipping, rejecting, and accepting all even and odd spins. This way, every lattice site is tested for a flip with each iteration. Therefore, the total number of complete iterations of the algorithm could be dramatically reduced by a factor of N . The system was taken through 1000 iterations of this procedure. A thermalization phase consisted of the first 30% iterations, in which the system could adjust to the parameters of the current simulation. After this phase, every iteration ended with computing both the magnetization and energy of the system. Finally, the mean magnetization and energy were computed, denoted $\langle m \rangle$ and $\langle E \rangle$. These values were then divided by the system size, N , to form a magnetization and energy density, as in $\frac{\langle m \rangle}{N}$ and $\frac{\langle E \rangle}{N}$. This allowed the results of the simulation to be compared with differently sized systems. The systems were subjected to different temperature spans and varying degrees of external magnetic fields. Furthermore, various system sizes were investigated.

2.2 Analytical Methods

Results were also gathered from two analytical methods: the mean-field theory, seen in Equation (13), and the exact solution in one dimension, as seen in Equation (14). However, in the mean-field approximation, m is both on the left and right sides of the equation and must be computed numerically. By repeatedly using a starting value and comparing with the result, an approximation of m could be determined using the fixed point algorithm, see Algorithm 1.

Algorithm 1: Computing magnetization with mean-field theory.

```
 $m_i = \text{initial value};$   
while  $|m_{i+1} - m_i| > \epsilon$  do  
   $m_{i+1} = \tanh\left(\frac{2Jm_i+h}{T}\right);$   
   $m_i = m_{i+1}$   
end  
return  $m_{i+1}$ 
```

3 Results

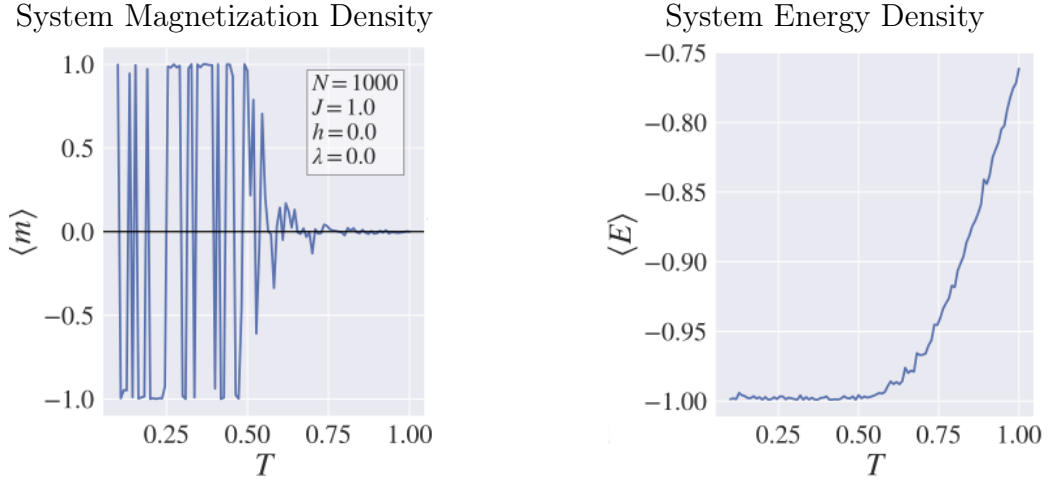
This section presents the results from running Monte-Carlo simulations over different temperature spans, using various external magnetic field strengths, and comparing them with analytical methods. All simulations in sections 3.2, 3.3, and 3.4 use an open boundary condition.

3.1 A Note on Units

For this report, the Boltzmann constant k_B has a value of one to simplify the mathematics and coding while still preserving the general properties of the Ising model. Therefore, the units of all computations are not standard SI units. The rest of this report will use only the numerical parts of the results.

3.2 Varying Temperatures without External Magnetic Fields

Figure 8 shows the results of the Monte Carlo simulations and analytical methods with no external magnetic field, $h = 0$. Solely the temperature is changed between rounds.



(a) The average magnetization density for different temperature values, $0 < T < 1$.

(b) The average energy density for different temperature values, $0 < T < 1$.

Figure 8: The average magnetization and energy density for varying temperatures without an external magnetic field.

As can be seen in Figure 8a, the average magnetization varies extensively. However, the magnetization stabilizes at zero for the temperature $T \approx 0.75$. The energy density graph is more expected; as the temperature increases, it provides the system with energy, causing the energy curve to grow. The results are very different when comparing with the exact solution and the mean-field theory, as seen in Figure 9.

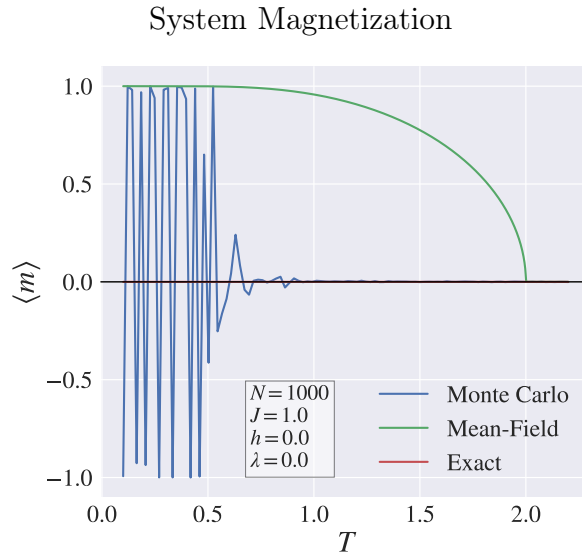
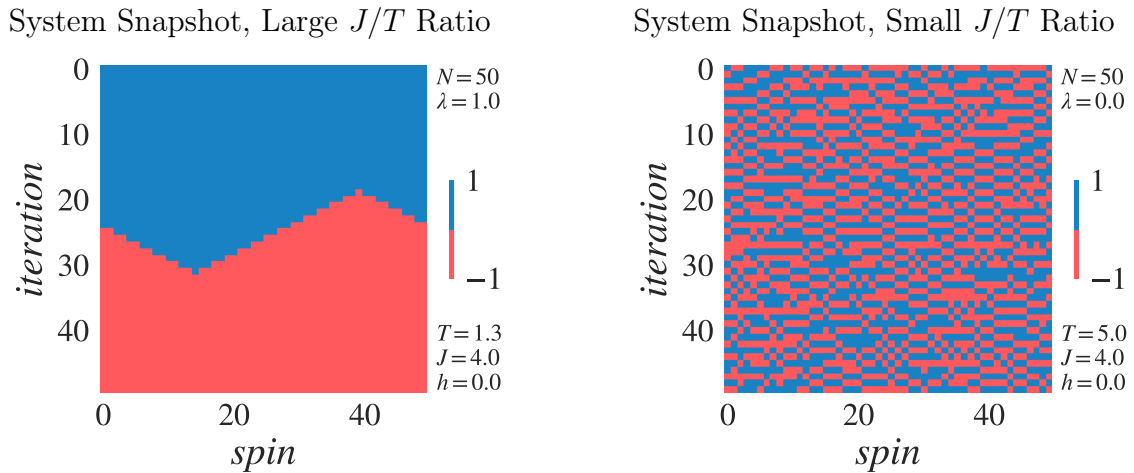


Figure 9: The average magnetization of a system of size $N = 1000$ with no external magnetic field, as predicted by Monte Carlo simulations (blue), mean-field theory (green), and the exact analytical solution of the one-dimensional Ising model (red).

The rapid change in magnetization can be closely observed in small systems, as seen in figures 10a and 10b. Every pixel represents the state of a spin at a specific lattice site. A blue pixel indicates an upward spin, while a red pixel indicates a downward spin. In essence, this forms a system snapshot, and the vertical axis makes it possible to track its evolution over the simulation.



(a) A relatively large J to T ratio. It suffices for one spin to change direction for every other spin to flip, as seen in the middle of the above system snapshot.

(b) A relatively small J to T ratio. The temperature constantly causes spins to flip, which leads to a disordered system state.

Figure 10: Snapshots of systems of size $N = 50$. Blue pixels represent upward spins, while red pixels represent downward spins.

3.3 Varying Temperatures with External Magnetic Fields

Figure 11 shows the results from exposing the system to an external magnetic field of strength $h = 0.5$. In this case, both the Monte Carlo simulations and analytical methods agree well with each other.

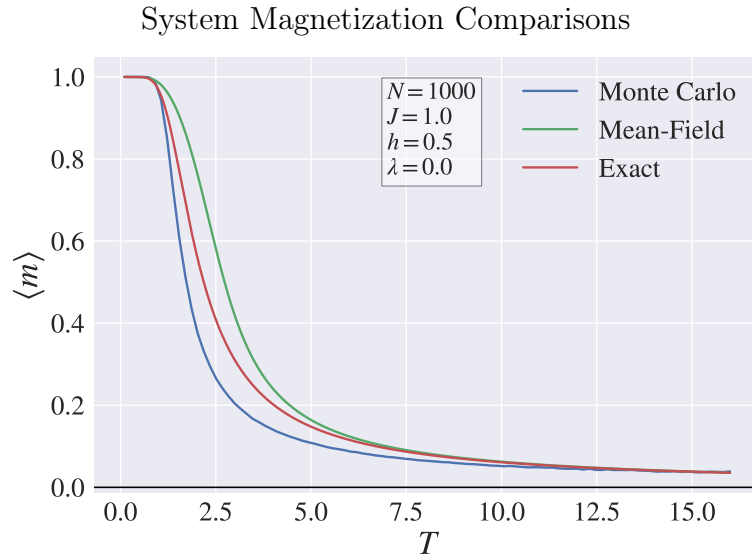
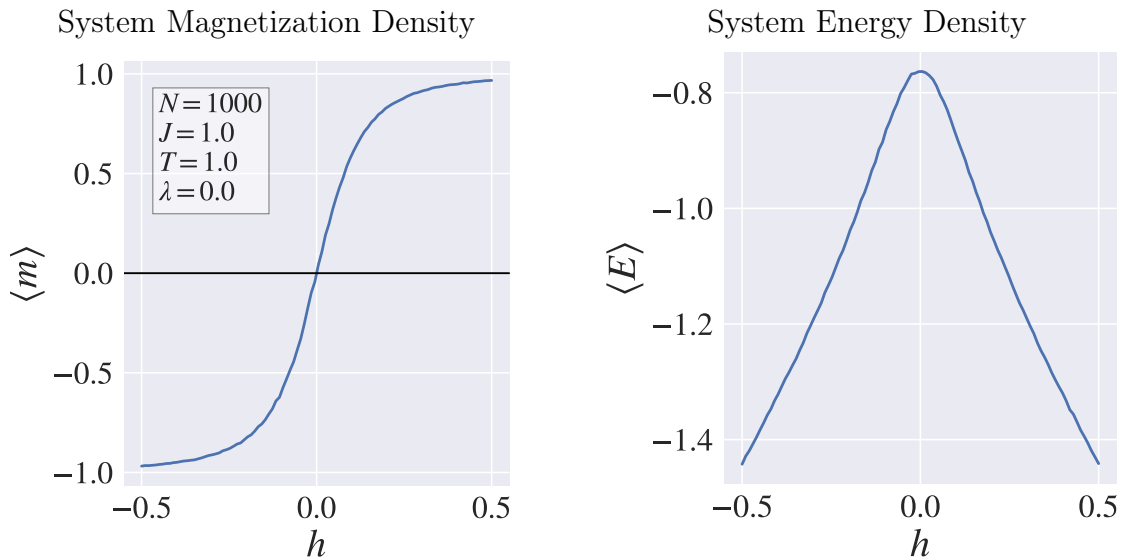


Figure 11: The average magnetization of a system of size $N = 1000$ with the presence of an external magnetic field, as predicted by Monte Carlo simulations (blue), mean-field theory (green), and the exact analytical solution of the one-dimensional Ising model (red).

3.4 Varying External Magnetic Field

Figure 12 shows only the results for a varying external magnetic field from the Monte Carlo simulations.



(a) The average magnetization density for varying external magnetic field strengths.

(b) The average energy density for varying external magnetic field strengths.

Figure 12: The average magnetization and energy density at the presence of an external magnetic field varying in field strength.

The comparisons between the different methods are shown in Figure 13. In this case, the Monte Carlo results agree with the exact analytical solution of the one-dimensional Ising model. The mean-field approximation works relatively well as it also conforms to the external magnetic fields. However, it is more extreme and steeper than the other two methods, rapidly changing magnetization around $h = 0$.

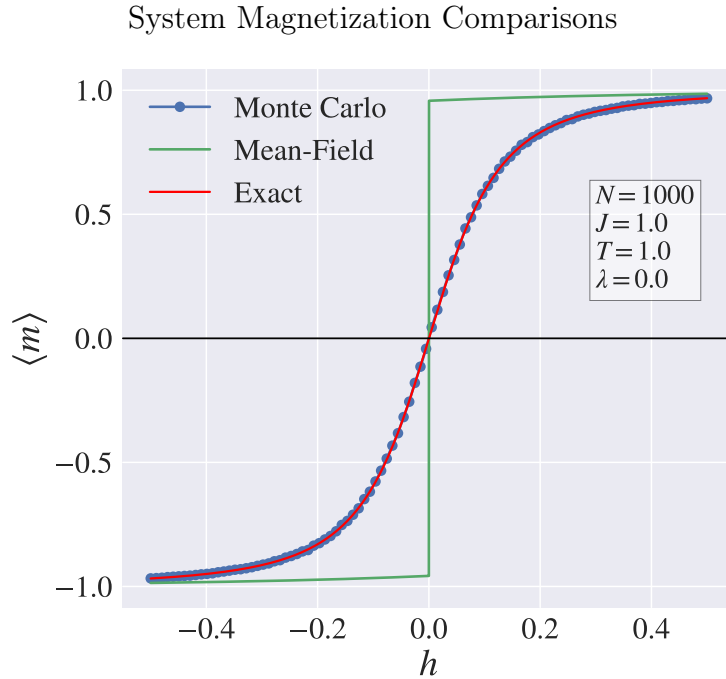


Figure 13: The average magnetization of a system of size $N = 1000$ at the presence of a varying external magnetic field, as predicted by Monte Carlo simulations (blue), mean-field theory (green), and the exact analytical solution of the one-dimensional Ising model (red).

3.5 Small Systems of Size $N < 100$

As discussed in the Introduction, the free energy could indicate when the system is prone to flip or not. For large systems in one dimension, F will always be negative, as the rightmost term will grow indefinitely while $2J$ stays constant, see (17).

$$\Delta F = 2J - k_B T \log(N - 1) \implies \lim_{N \rightarrow \infty} \Delta F < 0. \quad (17)$$

This is why the exact solution always yields zero magnetization in the absence of an external magnetic field. However, the free energy could be positive for minuscule system sizes. Figure 14 displays the values of ΔF for different system sizes and temperatures with various interspin exchange constants.

Free Energies for Varying Temperatures and System Sizes

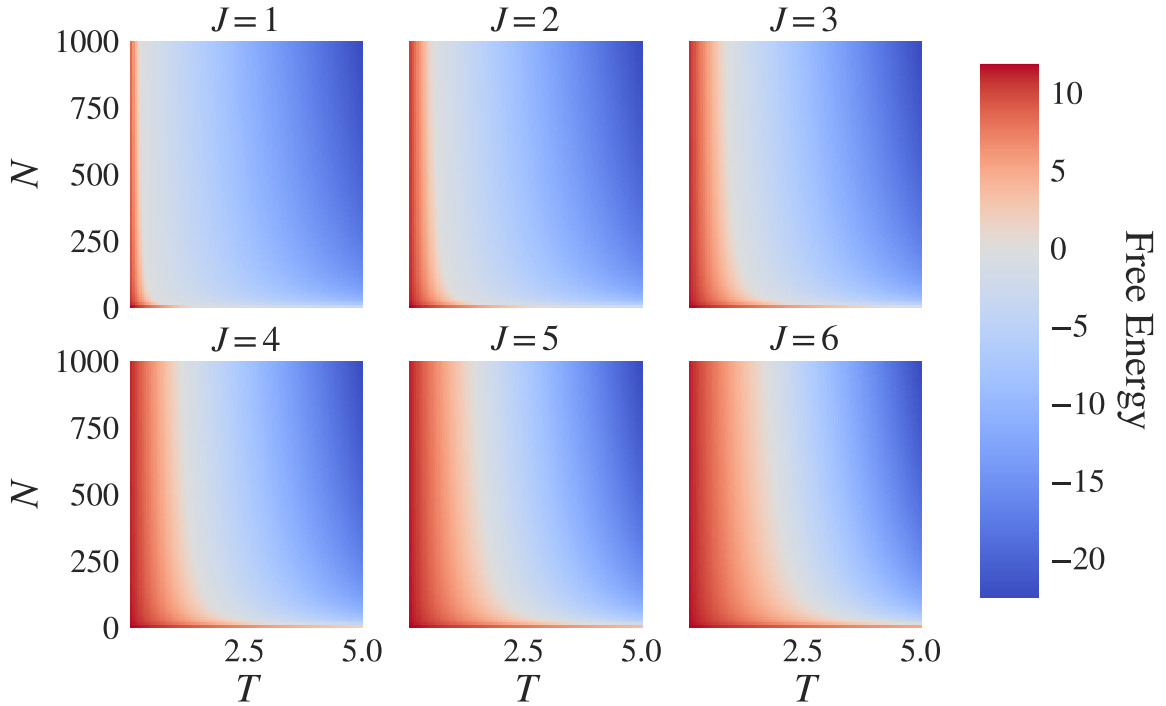
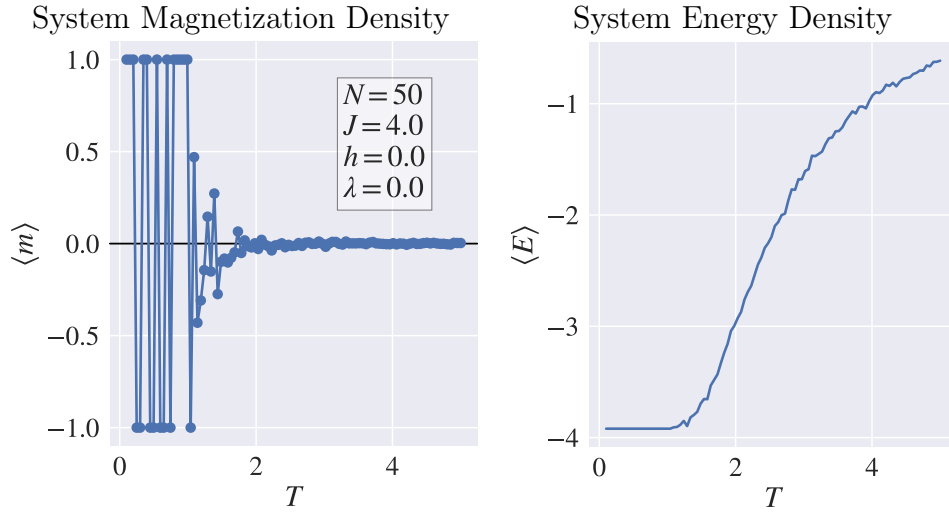


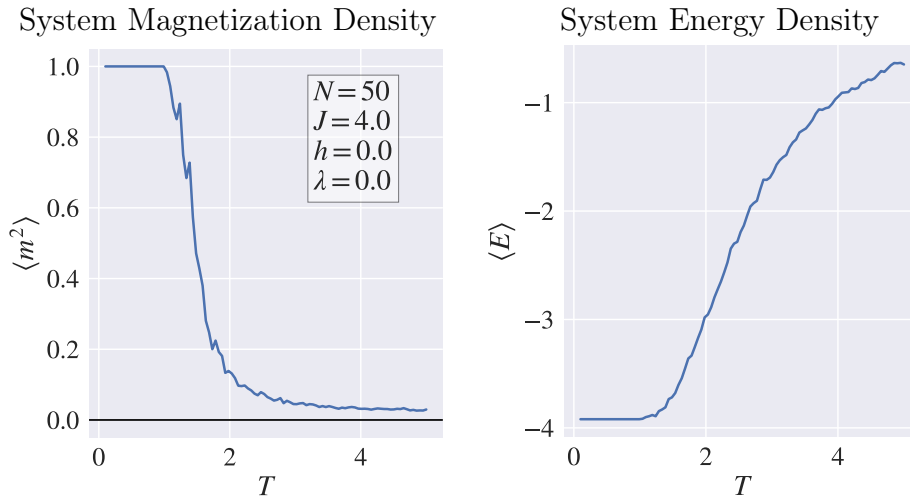
Figure 14: The free energy is computed at every point in the size-over-temperature graphs, represented as a color. The results are compared for different values of the interspin exchange constant J .

Using $N = 50$ and $J = 4$, a similar graph as in Figure 8 was produced, as seen in Figure 15. Although the magnetization constantly changes direction, it is also interesting to solely investigate its magnitude. In both cases, all spins align, which makes the specific direction less important. Plotting $\langle m^2 \rangle$ assures the magnetization remains positive while still allowing it to reach zero at higher temperatures.



(a) The average magnetization density for $0 < T < 5$. (b) The average energy density for $0 < T < 5$.

Figure 15: The average magnetization and energy density for a small system, for varying temperatures without an external magnetic field.



(a) The average magnetization density squared for $0 < T < 5$. (b) The average energy density for $0 < T < 5$.

Figure 16: The average magnetization density squared and energy density for a small system, for varying temperatures without an external magnetic field.

Magnetization, Specific Heat, and Magnetic Susceptibility

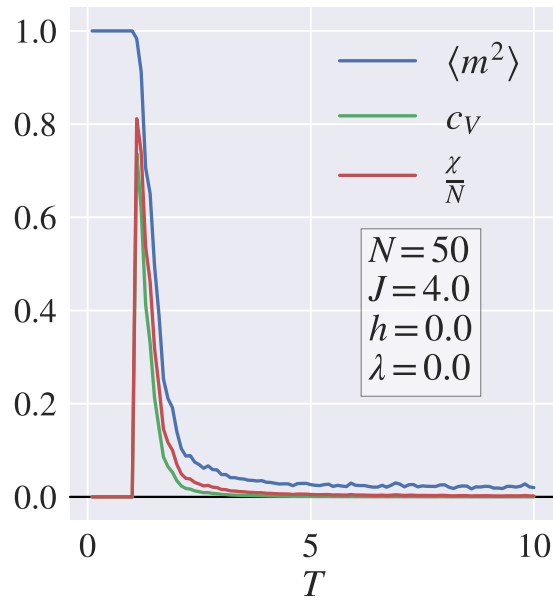
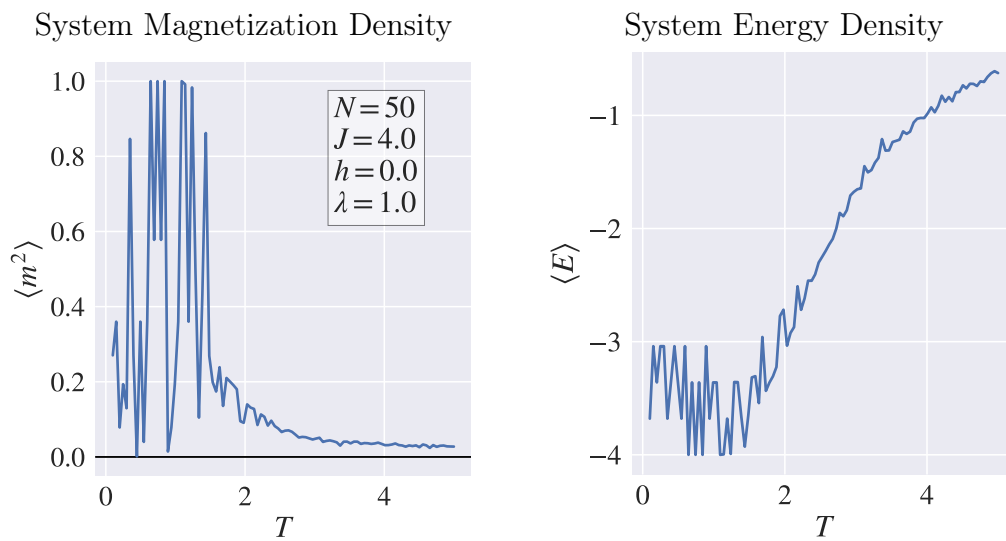


Figure 17: The graphs for specific heat, c_v , and magnetic susceptibility density, $\frac{\chi}{N}$, reach their peaks at the moment of rapid decrease of the magnetization graph.



(a) The average magnetization density squared for $0 < T < 5$.

(b) The average energy density for $0 < T < 5$.

Figure 18: The average magnetization density squared and energy density for a small system with the periodic boundary condition.

4 Discussion

As shown in Figure 9, the exact solution for an infinite system is zero regardless of temperature. The mean-field approximation does not seem accurate in this situation, as it begins with a magnetization of one and does not reach zero until $T = 2$. Why this happens is because mean-field assumptions fail in one-dimensional systems. As stated in the Introduction, the mean-field theory ignores fluctuations around the magnetization average. It works better in higher-dimensional systems where interactions between neighbors become more significant than thermal fluctuations. However, these fluctuations dominate in one-dimensional systems and force them into antiferromagnetic states, which results in faulty predictions by the mean-field approximation.

Although the Monte Carlo simulations show odd behavior at low temperatures, they agree well with the exact solution for higher temperatures. Still, there are some possible explanations as to why these sharp fluctuations appear. At low temperatures, the ratio between the interspin exchange constant J and the temperature T is comparatively large. On the one hand, this means that the interactions between the spins become more significant, as the temperature has a relatively small influence on the system. Therefore, they could overpower the energy, otherwise trying to force the system into an antiferromagnetic state, explaining why the system manages to stay magnetized. On the other hand, as the interactions between the spins are so strong, it suffices for one spin to flip to start a chain reaction that forces all others to change direction, see Figure 10a. For higher temperatures, the J to T ratio lowers, and the extra energy from the temperature dominates, forcing the system to repeatedly create domain walls, see Figure 10b.

In the case of an external magnetic field, seen in Figure 11, all methods agree well with each other. Therefore, both the mean-field approximation and Monte Carlo simulations seem to work under these conditions. At relatively low temperatures, the external magnetic field forces the spins to align with it, resulting in magnetization of the system. As the temperature increases, however, more magnetic moments start to flip. When the

spins point in different directions, the magnetization of the system lowers. At $T \approx 15$, the system reaches an antiferromagnetic state of complete opposite spins and zero magnetization.

Figure 12 shows a very symmetrical behavior. When the external magnetic field is negative, all spins point downwards, causing a negative magnetization. As the strength of the magnetic field approaches zero, so does the magnetization. Eventually, the magnetization reaches an expected value of zero at the removal of the external magnetic field. When the external magnetic field is positive, all spins instead point upwards, causing a positive magnetization. The energy graph is also symmetrical. When the external magnetic field is strong, it forces all spins to align. This is analogous to the ground state and requires the least amount of energy to maintain. As the strength of h subsides, the spins become more disordered, which increases the energy. The system is as most disordered at $h = 0$ when the absolute magnetization is at its lowest. The energy decreases as the external magnetic field once again increases in strength.

4.1 Small Systems of Size $N < 1000$

As seen in Figure 16, the magnetization of the smaller system is very similar to Figure 11, which included an external magnetic field. The specific heat and magnetic susceptibility suggest a critical temperature at the exact point where the magnetization starts to decline, as can be seen in Figure 17. These results indicate that small systems do have a critical temperature and a spontaneous magnetization below it. However, with the periodic boundary condition, the magnetization follows a similar path as for the larger systems, as seen in Figure 18, coherently with the use of periodic boundary conditions to simulate infinite systems. In this case, the change in free energy will always be negative, forcing the system to flip spins. Therefore, the magnetization becomes more sporadic than before and quickly reaches zero.

4.2 Limitations

There are possible limitations to this study. As an example, the Monte Carlo simulation did not seem to converge in specific cases. Either it is necessary to use more iterations or modify the algorithm. For instance, sampling from $e^{-dE/T}$ for low temperatures results in very small or large values which, compared with r , will either always reject or accept flips. How the magnetization varies over iterations can be seen in Figure 19 in the Appendix. As a final note, this report solely investigated systems of size $N \leq 1000$. To further examine the free energy for systems approaching infinite spins, it would be preferable to experiment with larger Ising models of $N \gg 1000$.

4.3 Applications and Further Development

According to the exact solution from Equation (14), one-dimensional systems do not experience spontaneous magnetization without an external magnetic field. Therefore, systems approaching infinite size do not undergo a phase transition as they enter an antiferromagnetic state for all temperatures above zero. However, models of adequately small sizes still have the potential to show these types of behavior. Their relatively modest computational load makes it possible to experiment with basic magnetic properties quickly and inexpensively. The model is also a foundation upon which more complicated models can be built. For example, many physical properties of one-dimensional systems transfer into higher dimensions.

As a further development, it would be intriguing to change more parameters. For example, would the system display similar behavior if it could interact with neighbors two or three lattice sites away? Similarly, investigating how multiple one-dimensional systems interact could also provide insights into how these systems behave. Moreover, could sociology and the Ising model be tied together to show similarities between how, for example, people adapt themselves and their opinions in response to their surroundings? All these questions are subject to exploration and research into this versatile model.

References

- [1] Plischke M, Bergersen B. Equilibrium Statistical Physics. 3rd ed. WORLD SCIENTIFIC; 2006. Available from: <https://www.worldscientific.com/doi/abs/10.1142/5660>.
- [2] Newman MEJ, Barkema GT. Monte Carlo Methods in Statistical Physics. Oxford: Oxford University Press; 1999.
- [3] Shackelford JF. 14. In: Introduction to materials science for engineers — Eighth Edition. Pearson; 2005. p. 526–557.
- [4] Widom B. 1. In: Statistical Mechanics: A Concise Introduction for Chemists. Cambridge: Cambridge University Press; 2002. p. 1–10.
- [5] Watkins JC. 2. In: An Introduction to the Science of Statistics: From Theory to Implementation. University of Arizona; 2016. p. 22–23.
- [6] Chib S, Greenberg E. Understanding the Metropolis-Hastings Algorithm. The American Statistician. 1995;49(4):327–335. Available from: <https://www.tandfonline.com/doi/abs/10.1080/00031305.1995.10476177>.
- [7] Singh SP. 1. In: Solid State Physics - Metastable, Spintronics Materials and Mechanics of Deformable Bodies. IntechOpen; 2020. p. 1–19.
- [8] Gong M, Wen X, Sun G, Zhang DW, Lan D, Zhou Y, et al. Simulating the Kibble-Zurek mechanism of the Ising model with a superconducting qubit system. Scientific Reports. 2016;6. Available from: <https://doi.org/10.1038/srep22667>.
- [9] Stauffer D. Social applications of two-dimensional Ising models. American Journal of Physics. 2008;76(4). Available from: <http://dx.doi.org/10.1119/1.2779882>.
- [10] Cervera-Lierta A. Exact Ising model simulation on a quantum computer. Quantum. 2018;2. Available from: <http://dx.doi.org/10.22331/q-2018-12-21-114>.

A Appendix

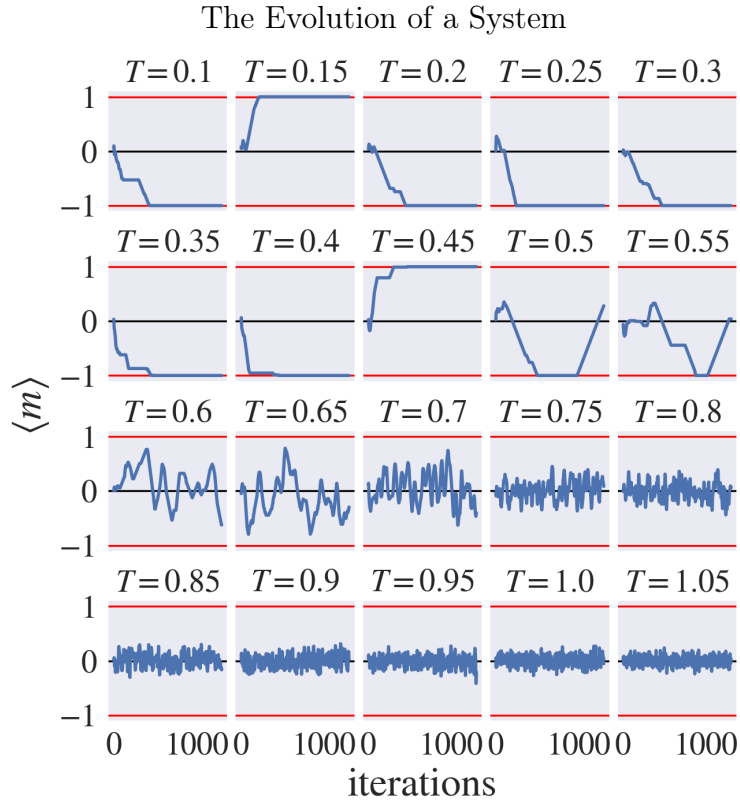


Figure 19: How the magnetization varies during the iterations of the Metropolis-Hastings algorithm for different values of T . In this experiment, $N = 1000$, $\lambda = 0$, $h = 0$, and $J = 1$.

System Snapshots

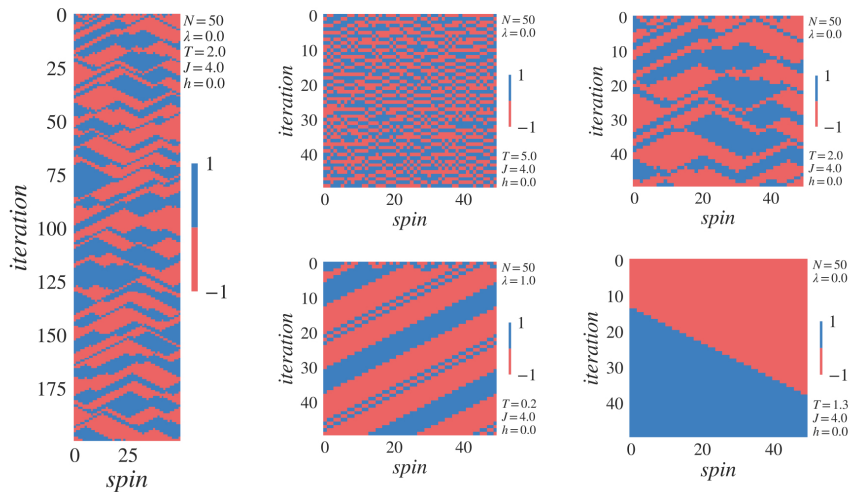


Figure 20: Various system snapshots of a system of size $N = 50$ for different values of T .